

Use CT Imaging to Predict the Short-Term Outcome of Concurrent Chemoradiotherapy in Patients With Locally Advanced Esophageal Squamous Cell Carcinoma

Xiaolan Cao^{1,2} , Xindi Li³, Xiaoyue Wang², Jinghao Duan², Shouhui Zhu², Haiyan Zeng², Yong Yin², Shuanghu Yuan², and Xudong Hu²

Abstract

Objective: To extract the computed tomography (CT) imaging features of the primary lesions in patients with advanced esophageal squamous cell carcinoma (ESCC) and to study whether these imaging features can predict the short-term outcome after concurrent chemoradiotherapy (CCRT).

Methods: From January 2014 to December 2015, a total of 49 patients with locally advanced ESCC who underwent CCRT were analyzed retrospectively. They were randomly categorized into the training and validation groups. Collection of CT imaging of patients before and intermediate stage undergoing radiotherapy. The correlations between imaging characteristics and short-term outcome were analyzed. The accuracy of cutoff value was verified by imaging characteristics of patients in validation group.

Result: There were 38 patients in the training group and 11 patients in the validation group. 13 patients in the training group were classified as responders and 25 patients as nonresponders. According to the CT imaging before radiotherapy, there are no significant differences between responders and nonresponders. According to the CT imaging in the middle stage of radiotherapy, responders showed significantly higher Roundness than nonresponders ($P = .004$, 95% confidence interval [CI] = 0.0419-0.212). The areas under the ROC curves for the ability to predict significantly tumor response were 0.768 for Roundness ($P = .001$, 95% CI = 0.603-0.889). The cutoff value of Roundness is 0.3099. Roundness showed no significant associations with survival parameters.

Conclusions: Computed tomography imaging in the middle stage of radiotherapy can predict the short-term outcome of concurrent chemoradiotherapy for patients with locally advanced ESCC but have no predictive effect on the total survival time.

Keywords

esophageal squamous cell carcinoma, short-term outcome, CT imaging, chemoradiotherapy

¹ School of Medicine and Life Sciences, University of Jinan, Jinan, China

² Department of Radiation Oncology, Shandong Cancer Hospital and Institute, Shandong First Medical University and Shandong Academy of Medical Sciences, Jinan, China

³ Department of Oncology, Shandong Provincial Third Hospital, Jinan, China

Received 21 August 2019; received revised 17 November 2019; accepted 1 December 2019

Corresponding Author:

Xudong Hu, Department of Radiation Oncology, Shandong Cancer Hospital and Institute, Shandong First Medical University and Shandong Academy of Medical Sciences, 440 Jijian Road, Jinan, Shandong Province, China 250117.

Email: drhuxudong@163.com



Creative Commons Non Commercial CC BY-NC: This article is distributed under the terms of the Creative Commons Attribution-NonCommercial 4.0 License (<https://creativecommons.org/licenses/by-nc/4.0/>) which permits non-commercial use, reproduction and distribution of the work without further permission provided the original work is attributed as specified on the SAGE and Open Access pages (<https://us.sagepub.com/en-us/nam/open-access-at-sage>).

Introduction

China is one of the countries with a high incidence of esophageal cancer, and it has the highest number of patients with esophageal cancer in the world.¹ Although surgical resection provides a chance of cure, 80% of patients with esophageal cancer have unresectable disease at the time of diagnosis, will need radiotherapy and chemotherapy. Radiotherapy is an important treatment for patients with advanced esophageal cancer.² In clinical practice, the sensitivity to radiotherapy and chemotherapy or prognosis of patients vary even in patients with the same stage of disease, with the same pathological type and after the same treatment methods. Using effective imaging and biological indicators may help clinicians to formulate individualized treatment strategies to improve the survival of patients with esophageal squamous cell carcinoma (ESCC).

Radiomics has emerged as a promising approach in the discovery of quantitative imaging biomarkers in patients with cancers.³ The basic principle of radiomics is that by extracting a large number of hypothetical imaging features, we can obtain a more comprehensive description of potential tumor phenotypes, which may be associated with clinical outcomes. Computed tomography (CT) imaging analysis is a potential independent biomarker of malignancy. This approach has been used to predict the overall survival in patients with lung cancer using widely available imaging techniques.^{4,5} Imaging analysis reflects the heterogeneity of a tumor,⁶⁻¹⁰ which manifests as cell infiltration, abnormal vascular proliferation, fine structure, and necrosis.¹¹⁻¹³ Studies have shown that certain imaging features are associated with tumor glycometabolism and grading,¹⁴ as well as with hypoxia and angiogenesis.⁹ Multiple studies have reported that metabolic tumor volume is a prognostic factor in patients with non-small cell lung cancer.¹⁵⁻¹⁷ In this clinical study, we investigated whether CT imaging can be used to predict treatment response after concurrent chemoradiotherapy (CCRT) in patients with advanced ESCC.

Materials and Methods

Study Population

The patients with locally advanced ESCC were eligible for this study between January 2014 and October 2015. All patients met the following inclusion criteria: (1) Locally advanced ESCC confirmed by pathology diagnosis, (2) Karnofsky performance status ≥ 70 , and (3) had measurable primary tumors according to the Response Evaluation Criteria in Solid Tumors (RECIST version 1.1). Patients treated with any surgical resection were excluded.

Treatment and Response Assessment

Patients were treated with CCRT. Radiation therapy was delivered using intensity-modulated radiotherapy or 3-dimensional conformal radiation therapy. Treatment was administered using a conventionally fractionated regimen of 1.8 to 2.0 Gy for 5 days a week. The total dose administered to patients ranged

from 56 to 66 Gy (median, 60 Gy). At least 1 month after completion of the treatment, patients were reassessed to determine response to therapy using the CT. Computed tomography imaging analysis of patients at simulation before radiotherapy, mid-radiotherapy, and after radiotherapy were collected, respectively.

Imaging Analysis

Computed tomography imaging before and in the middle stage of radiotherapy were analyzed, respectively. A total of 76 quantitative features including morphologic features, statistical features, histogram-related features, and imaging features were calculated from CT texture of each patient. These imaging features may provide a more comprehensive characterization of the underlying tumor phenotypes. We investigated 3 types of imaging features on the basis of gray-level co-occurrence matrices,¹⁸ wavelet decompositions,¹⁹ and Laws features.²⁰ To meaningfully characterize tumors, all imaging features were further processed to be rotationally invariant (without preference to any particular spatial direction). The calculation of all imaging features was performed using IBEX software. This software runs on a Windows-based personal computer and can analyze imaging in the digital imaging and communications in medicine format (the most commonly used file format in medical imaging and radiology practice). The IBEX software can be integrated with a picture archiving and communication system or run as standalone imaging analysis software.

For a gray-level co-occurrence matrix with size $N_g \times N_g$, it describes the second-order joint probability function of an imaging region and is defined as $P(i, j | \delta, \theta)$. Let:

N_g be the number of discrete gray level within imaging.

$P(i, j)$ be the co-occurrence matrix for an arbitrary δ and θ and.

$$\text{Entropy} = - \sum_{i,j} i, j P(i, j) \log P(i, j);$$

$$\text{Dissimilarity} = \sum_{i=1}^{N_g} \sum_{j=1}^{N_g} |i - j| p(i, j),$$

$$\text{Homogeneity} = \sum_{i=1}^{N_g} \sum_{j=1}^{N_g} \frac{p(i, j)}{1 + |i - j|}.$$

Entropy reflects irregularity in the gray-level co-occurrence matrix, and a completely random distribution would have very high entropy. Dissimilarity is a measure that defines the variation of gray-level pairs in an imaging. Homogeneity measures the uniformity of the gray-level co-occurrence matrix. Max3D Diameter: Largest pairwise Euclidean distance between voxels on the surface of the tumor volume. Roundness represents the ratio of the surface area of a sphere of the same volume as an object to the surface area of an object.

Response Evaluation

Patients were reassessed for treatment response by CT imaging at 1 month after completion of the treatment. Tumor response was subsequently classified as complete response (CR), partial

Table 1. Characteristics of Patients (n = 49).

Characteristic	No. of Patients(%)	P Value
Age, years	62 ± 20	.428
<65	30 (61.2%)	
≥65	19 (38.8%)	
Sex		1
Male	32 (65.3%)	
Female	17 (34.7%)	
Stage		.124
IIIA	12 (24.5%)	
IIIB	26 (53.1%)	
IVA	11 (22.4%)	
Pathologic		
Squamous cell carcinoma	49 (100%)	
Primary site		.267
Upper esophagus	12 (24.5%)	
Middle esophagus	22 (44.9%)	
Lower esophagus	15 (30.6%)	

response (PR), stable disease (SD), or progressive disease (PD) according to the RECIST (version 1.1). Patients with CR or PR were considered as responders, and patients with SD or PD as nonresponders.

Statistical Analysis

χ^2 test was used to test the significance of the primary tumor and lymph node status and the stage with the treatment response. The correlation between imaging characteristics and short-term outcome was analyzed by *t* test, and receiver operating characteristic (ROC) curve was used to evaluate the predictive ability of imaging characteristics and the determination of cutoff value. The accuracy of cutoff value was verified by imaging characteristics of patients in the validation group. The correlation with survival time was evaluated by Kaplan–Meier analysis.

A value of $P < .05$ was considered as statistically significant and all P values presented are 2-sided. The statistical analyses were performed using the MedCalc Statistical Software and GraphPad Prism Statistical Software.

Results

Patient and Tumor Characteristics

Forty-nine patients (32 males, 17 females; range, 49–86 years) were eligible for the analysis. All tumors were squamous cell carcinoma. Most of them originated from the middle and lower esophagus (76%). All patients were diagnosed with locally advanced ESCC (Table 1).

A total of 76 imaging group features were extracted, including 18 size and shape features, 18 histogram intensity features, and 40 texture features (Table 2). Firstly, the 76 imaging features were extracted, and then *t* test was used to analyze the correlation between imaging features and short-term curative effect. Finally, only 1 imaging feature was included in the follow-up analysis.

Table 2. Detailed Imaging Features.

Size and shape	Maximum 3D diameter, compactness 2, maximum 2D diameter, slice, maximum 2D diameter row, maximum 2D diameter column, volume, surface volume ratio, surface area, sphericity, compactness 1, roundness, flatness, elongation, spherical disproportion, major axis, least axis, minor axis j
Histogram intensity	Interquartile range, minimum, standard deviation, entropy, variance skewness f, uniformity, 90 percentile, robust mean absolute deviation, mean absolute deviation, median, root mean squared, kurtosis, mean, energy, maximum, range, homogeneity
Texture features	Homogeneity 1, homogeneity 2, ldmn, difference entropy, ldn, ldm, sum variance, gluster shade, correlation, maximum probability, contrast, sum En, autocorrelation, difference average, cluster tendency, lmc 2, difference variance, inverse variance, dissimilarity, suxn average, run length nonuniformity, run length nonuniformity normalized, run percentage, short run emphasis, gray level emphasis, dissimilarity, zone variance, zone percentage, long run low gray level emphasis, gray level variance, run entropy, high gray level run emphasis, small area Hgh gray level emphasis, average intensity, gray level nonuniformity normalized, size zone nonuniformity, gray level nonuniformity, size zone non uniformity normalized, large area low gray level emphasis, large area emphasis

Tumor Response Prediction

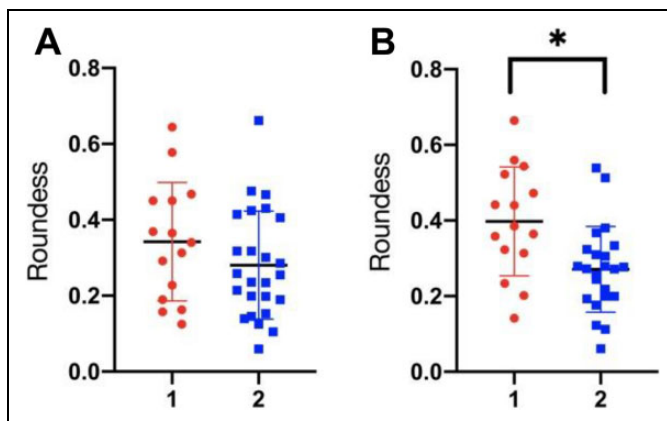
Forty-nine patients were randomly assigned, including 38 patients in the training group and 11 patients in the validation group. In the training group, there were 13 responders and 25 nonresponders. Univariate analysis of the relationship between clinicopathological factors and short-term outcome. Neither tumor status ($P = .122$) nor radiotherapy dose ($P = 0.112$) reached statistical significance with tumor response (Table 3).

The CT imaging characteristics were changed in different degrees before and after radiotherapy. The imaging characteristics of radiotherapy localization were analyzed. The correlation between imaging characteristics and short-term outcome was analyzed by *t* test, the results showed that there was no significant difference between responders and nonresponders ($P = .208$). Computed tomography imaging in the middle stage of radiotherapy were analyzed, the results showed that there was a significant difference in Roundness of imaging features between responders and nonresponders ($P = .004$). Comparison of Roundness between responders and nonresponders was shown in Figure 1.

The average value of Roundness in the responders and nonresponders were 0.34 and 0.28 in radiotherapy localization. The average sphericity of responders and nonresponders were 0.39 and 0.27 in the middle stage of radiotherapy. Other imaging characteristics are shown in Tables 4 and 5.

Table 3. Characteristics of Patients in the Experimental Group (n = 38).

Characteristic	Experiment			P Value
	I Group (n = 38)	Responders (n = 13)	Nonresponders (n = 25)	
T-stage distribution (T1/T2/T3/T4)	1/9/15/13	1/5/5/2	0/4/10/11	.122
Lymph nodal status (N0/N1/N2)	0/20/18	0/8/5	0/12/13	.428
Stage group (IIIA/IIIB/IVA)	9/15/14	4/3/6	5/12/8	.195
Radiotherapy dose (Gy) ≤56/ ≤60/ ≤66	2/10/26	0/6/7	2/4/19	.112
Chemotherapy				.493
PF (cisplatin + 5fluorourac)	19	7	12	
DP (docetaxel + cisplatin)	9	4	5	
DN (docetaxel + nedaplatin)	10	6	4	

**Figure 1.** Distribution of Roundness between responders and non-responders. A, Distribution of Roundness values during radiotherapy localization. Group 1 was the responders, and group 2 was the non-responders. B, Distribution of Roundness values in the middle stage of radiotherapy. Group 1 was the responders, and group 2 was the non-responders.**Table 4.** Comparison of CT Imaging Between Responders and Non-responders During Radiotherapy Localization.

Time	Parameters	Responders (n = 13)	Nonresponders (n = 25)	P Value
Radiotherapy localization	Max 3D Diameter	2.66 ± 0.67	3.04 ± 0.88	.098
	Entropy	4.64 ± 0.51	2.66 ± 0.68	.118
	Surface Area	7.74 ± 1.85	8.48 ± 2.29	.153
	Dissimilarity	1.23 ± 0.37	1.14 ± 0.32	.681
	Roundness	0.34 ± 0.15	0.28 ± 0.13	.208

Abbreviation: CT, computed tomography.

Table 5. Comparison of CT Imaging Between Responders and Nonresponders in the Middle Stage of Radiotherapy.

Time	Parameters	Responders (n = 13)	Nonresponders (n = 25)	P Value
Middle stage of radiotherapy	Max3D Diameter	2.54 ± 0.62	2.92 ± 0.76	.147
	Entropy	4.44 ± 0.49	3.62 ± 1.59	.285
	Surface Area	7.36 ± 1.81	8.41 ± 2.05	.279
	Dissimilarity	1.13 ± 0.35	1.15 ± 0.26	.443
	Roundness	0.39 ± 0.13	0.27 ± 0.11	.004

Abbreviation: CT, computed tomography.

Table 6. Areas Under ROC Curves for Ability of CT Imaging in the Middle Stage of Radiotherapy to Predict Response in Patients.

Parameters	Area Under ROC Curve		95% Confidence Intervals	Sensitivity	Specificity	P Value
	Area Under ROC Curve	95% Confidence Intervals				
Max 3D Diameter	0.635	0.463-0.785	93.3	34.8	.146	
Entropy	0.601	0.429-0.755	86.7	47.8	.285	
Surface Area	0.603	0.432-0.758	86.8	47.7	.279	
Dissimilarity	0.577	0.406-0.758	66.7	65.2	.443	
Roundness	0.768	0.603-0.889	80.1	73.9	.001	

Abbreviations: CT, computed tomography; ROC, receiver operating characteristic.

The areas under the ROC curves for the ability to predict significantly tumor response were 0.768 for Roundness ($P = .001$, 95% confidence interval = 0.603-0.889). Other imaging characteristics are shown in Table 6. The cutoff value of Roundness is 0.3099. If the value of Roundness is greater than 0.3099, then the patient is responder.

All 11 patients in the validation group received CT imaging examination before and 3 months after the treatment. Tumor response was subsequently classified as CR, PR, SD, or PD according to the RECIST version 1.1. Patients with CR or PR were considered as responders, and patients with SD or PD as nonresponders. According to the RECIST version 1.1, there were 5 responders and 6 nonresponders, but according to the cutoff value of Roundness, there were 4 responders and 7 nonresponders. The validation group of 10 patients according to the cutoff value of Roundness was consistent with the grouping based on the RECIST version 1.1. One patient is an exception, this patient is well treated, but the value of Roundness is less than 0.309. The therapeutic effect of this patient is shown in Figure 2. The roundness value distribution of responders and nonresponders is shown in Figure 3.

Survival Prediction

No differences are demonstrated in parameters. Kaplan–Meier survival curves of the overall survival (OS) demonstrate no

differences in patients with high and low Roundness (OS, $P = .6141$). Roundness showed no significant associations with survival parameters (Figure 4).

Discussion

In this study, ROC curve is used to find the cutoff value. According to the previously published literature and opinions of related statisticians, there are 2 common methods: One is screening through ROC curve, and the other is screening through Cox regression, and which one is more suitable? There still exists argument. Comparing these 2 methods, the ROC curve combines sensitivity and specificity with graphic methods and retains small differences in parameters between different patients, a feature which is a comprehensive representative of the accuracy of the test. While Cox regression analysis incorporates numerical variables, so it poses a risk of quantifying qualitative data and may indirectly reduce the effectiveness of the screening. As the ROC curve retains small differences in parameters between different patients, we selected it as our primary screening method.

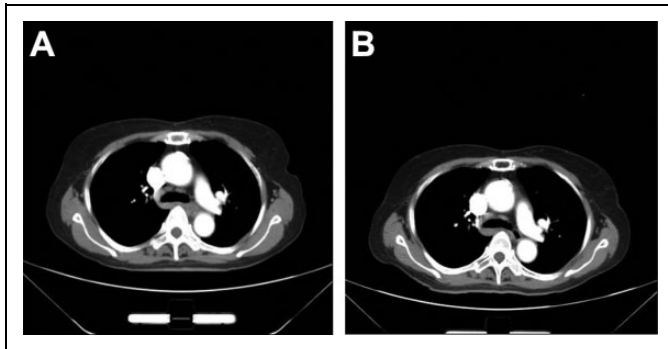


Figure 2. Computed tomography imaging of this patient before treatment (A) and after treatment (B).

The next question is the choice of critical point in imaging analysis: Should it be the dividing value of the ROC or the median? In order to distinguish the patient from the parameters of imaging analysis, the determination of the critical point is important. In this process, 2 methods are available for reference: One is the dividing value of ROC and the other is the median value of the imaging parameters. If the median grouping method is adopted, it will only represent the medium level of the data and will not represent the whole status. This may result in the significant reduction or even disappearance of the meaning of the population screening. According to our results, the differences between the 2 studies will be more significant when grouped by the dividing value. Therefore, we suggest the following recommendations: If the median grouping method fails to achieve effective differentiation among patients based on actual clinical outcomes, the dividing value of ROC should be considered as the basis.

The imaging features in this study are sphericity, which reflects the shape of the tumor. Computed tomography imaging can quantitatively analyze the characteristics of tumor tissue, and the volume and surface area of tumor can be calculated by extracting the shape features. From the ratio of surface area to volume (surface area/volume), it can be seen that when the volume is constant, the surface area of the sphere shape is the smallest, the edge has the shape of protuberance or burr, and its surface area increases. For example, the burr sign of the tumor is a manifestation of tumor invasion and growth, and the prognosis is usually poor.^{21,22} Other studies have confirmed that volume and maximum surface distance can be used to compare stability and accuracy.^{23,24} Kidd et al found that 4 image features (energy, contrast, entropy, and average degree) can be used to predict the efficacy of patients.²⁵ The effectiveness of each imaging feature is different, and the significance of each imaging feature is also different.

However, despite intensive investigation of these and other imaging metrics, the predictive value of these metrics to allow

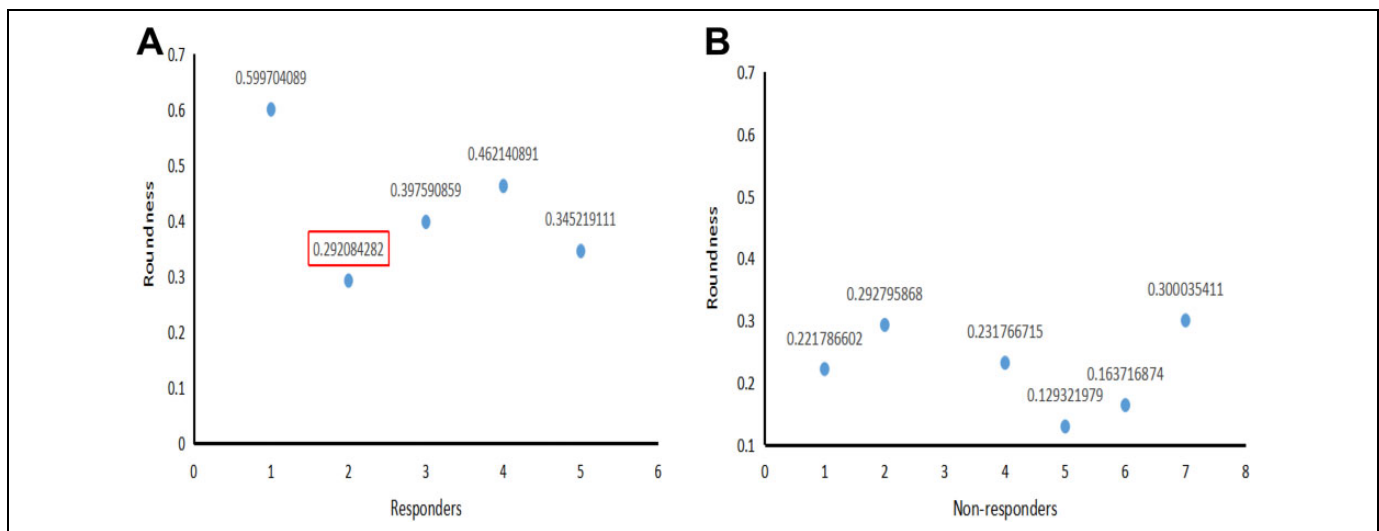


Figure 3. Distribution of Roundness values in responders (A) and nonresponders (B).

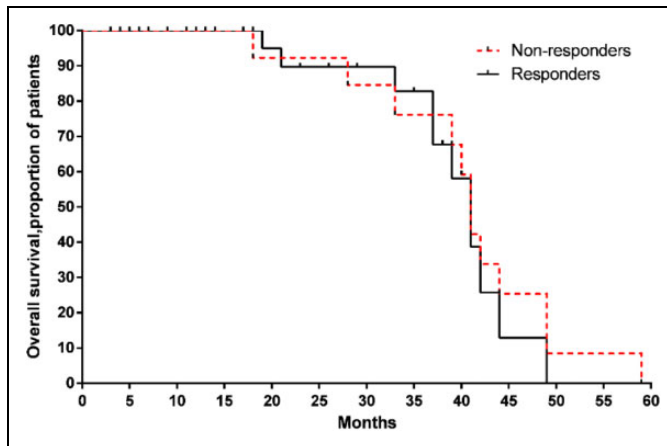


Figure 4. Survival analysis of Roundness in patients.

accurate discrimination between different risk groups appears to be limited. More sophisticated tools that improve on existing imaging metrics are needed. Some scholars extracted 219 image features from 2 sets of CT imaging scanned repeatedly at intervals of 15 minutes, and their repeatability was evaluated by intragroup correlation coefficient. The results show that only 30% (66) of the features are repetitive, and most of the image features are unstable.²⁶

The significance of this study is that the sensitivity of patients to radiotherapy can be evaluated according to the CT imaging in the middle stage of radiotherapy, to increase or decrease the radiotherapy dose. In the recovery radiotherapy, roundness has some predicted effects on the partial result to the late period of esophageal cancer, but it has no predicted effect on the total lifetime. Computed tomography imaging has some significant meanings to the radiotherapy to the late period of esophageal cancer. The results of this study need to be further verified using a multicenter prospective study and by including more imaging parameters, mathematical modeling, and machine learning to guide clinical treatment decisions.

Conclusions

Computed tomography imaging in the middle stage of radiotherapy can predict the short-term outcome of CCRT for patients with locally advanced ESCC but have no predictive effect on the total survival time.

Acknowledgements

The authors would like to thank Ms Feng-Ming (Spring) Kong for excellent assistance.

Author contribution

Xiaolan Cao and Xindi Li have contributed equally to this work.


Declaration of Conflicting Interests

The author(s) declared no potential conflicts of interest with respect to the research, authorship, and/or publication of this article.

Funding

The author(s) disclosed receipt of the following financial support for the research, authorship, and/or publication of this article: This work was supported by the Key R&D projects in Shandong Province [grant number 2017GSF2018044].

ORCID iD

Xiaolan Cao  <https://orcid.org/0000-0001-6380-1911>

References

- Garg PK, Sharma J, Jakhetiya A, Goel A, Gaur MK. Preoperative therapy in locally advanced esophageal cancer. *World J Gastroenterol.* 2016;22(39):8750-8759. doi:10.3748/wjg.v22.i39.8750.
- Kimura M, Ishiguro H, Tanaka T, Takeyama H. Advanced esophageal cancer with tracheobronchial fistula successfully treated by esophageal bypass surgery. *Int J Surg Case Rep.* 2015;9: 115-118. doi:10.1016/j.ijscr.2015.02.053.
- Kumar V, Gu Y, Basu S, et al. Radiomics: the process and the challenges. *Magn Reson Imaging.* 2012;30(9):1234-1248. doi:10.1016/j.mri.2012.06.010.
- Depeursinge A, Yanagawa M, Leung AN, Rubin DL. Predicting adenocarcinoma recurrence using computational texture models of nodule components in lung CT. *Med Phys.* 2015;42(4): 2054-2063. doi:10.1118/1.4916088.
- Aerts HJ, Velazquez ER, Leijenaar RT, et al. Decoding tumour phenotype by noninvasive imaging using a quantitative radiomics approach. *Nat Commun.* 2014;5:4006. doi:10.1038/ncomms5006.
- Goh V, Ganeshan B, Nathan P, Juttla JK, Vinayan A, Miles KA. Assessment of response to tyrosine kinase inhibitors in metastatic renal cell cancer: CT texture as a predictive biomarker. *Radiology.* 2011;261(1):165-171. doi:10.1148/radiol.11110264.
- Ganeshan B, Goh V, Mandeville HC, Ng QS, Hoskin PJ, Miles KA. Non-small cell lung cancer: histopathologic correlates for texture parameters at CT. *Radiology.* 2013;266(1):326-336. doi:10.1148/radiol.12112428.
- Ng F, Ganeshan B, Kozarski R, Miles KA, Goh V. Assessment of primary colorectal cancer heterogeneity by using whole-tumor texture analysis: contrast-enhanced CT texture as a biomarker of 5-year survival. *Radiology.* 2013;266(1):177-184. doi:10.1148/radiol.12120254.
- Zhang H, Graham CM, Elci O, et al. Locally advanced squamous cell carcinoma of the head and neck: CT texture and histogram analysis allow independent prediction of overall survival in patients treated with induction chemotherapy. *Radiology.* 2013; 269(3):801-809. doi:10.1148/radiol.13130110.
- Yip C, Landau D, Kozarski R, et al. Primary esophageal cancer: heterogeneity as potential prognostic biomarker in patients treated with definitive chemotherapy and radiation therapy. *Radiology.* 2014;270(1):141-148. doi:10.1148/radiol.13122869.
- Davnall F, Yip CS, Ljungqvist G, et al. Assessment of tumor heterogeneity: an emerging imaging tool for clinical practice. *Insights Imaging.* 2012;3(6):573-589. doi:10.1007/s13244-012-0196-6
- Lunt SJ, Chaudary N, Hill RP. The tumor microenvironment and metastatic disease. *Clin Exp Metastasis.* 2009;26(1):19-34. doi: 10.1007/s10585-008-9182-2.

13. Ganeshan B, Panayiotou E, Burnand K, Dizdarevic S, Miles K. Tumour heterogeneity in non-small cell lung carcinoma assessed by CT texture analysis: a potential marker of survival. *Eur Radiol.* 2012;22(4):796-802. doi:10.1007/s00330-011-2319-8.
14. Ganeshan B, Abaleke S, Young RC, Chatwin CR, Miles KA. Texture analysis of non-small cell lung cancer on unenhanced computed tomography: initial evidence for a relationship with tumour glucose metabolism and stage. *Cancer Imaging.* 2010; 10:137-143. doi:10.1102/1470-7330.2010.0021.
15. Meng X, Sun X, Mu D, et al. Noninvasive evaluation of microscopic tumor extensions using standardized uptake value and metabolic tumor volume in non-small-cell lung cancer. *Int J Radiat Oncol Biol Phys.* 2012;82(2):960-966. doi:10.1016/j.ijrobp.2010.10.064.
16. Liao S, Penney BC, Wroblewski K, et al. Prognostic value of metabolic tumor burden on 18F-FDG PET in nonsurgical patients with non-small cell lung cancer. *Eur J Nucl Med Mol Imaging.* 2012;39(1):27-38. doi:10.1016/j.acra.2011.08.020.
17. Abelson JA, Murphy JD, Trakul N, et al. Metabolic imaging metrics correlate with survival in early stage lung cancer treated with stereotactic ablative radiotherapy. *Lung Cancer.* 2012;78(3): 219-224. doi:10.1016/j.lungcan.2012.08.016.
18. Haralick RM, Shanmugam K, Dinstein IH. Textural features for image classification. *Stud Media Comm.* 1973;3(6):610-621. doi:10.1109/TSMC.1973.4309314.
19. Mallat SG. A theory for multiresolution signal decomposition: the wavelet representation. *IEEE Trans Pattern Anal Mach Intell.* 1989;11(7):674-693. doi:10.1109/34.192463.
20. Kuglin CD, Eppler WG. Map-matching techniques for use with multispectral/multitemporal data//image processing for missile guidance. *Int Soc Optics Photon.* 1980;238:146-155. doi:10.1117/12.959141.
21. Honda T, Kondo T, Murakami S, et al. Radiographic and pathological analysis of small lung adenocarcinoma using the new IASLC classification. *Clin Radiol.* 2013;68(1):e21-e26. doi:10.1002/mp.12901.
22. Grove O, Berglund AE, Schabath MB, et al. Quantitative computed tomographic descriptors associate tumor shape complexity and intratumor heterogeneity with prognosis in lung adenocarcinoma. *PLoS One.* 2015;10(3):e0118261. doi:10.1371/journal.pone.0118261.
23. Warfield SK, Zou KH, Wells WM. Simultaneous truth and performance level estimation(STAPLE): an algorithm for the validation of image segmentation. *IEEE Trans Med Imaging.* 2004; 23(7):903-921. doi:10.1109/TMI.2004.828354.
24. Jameson MG, Holloway LC, Vial PJ, et al. A review of methods of analysis in contouring studies for radiation oncology. *J Med Imaging Radiat Oncol.* 2010;54(5):401-410. doi:10.1111/j.1754-9485.2010.02192.
25. Kidd EA, El NI, Siegel BA, et al. FDG-PET-based prognostic nomograms for locally advanced cervical cancer. *Gynecol Oncol.* 2012;127(1):136-140. doi:10.1016/j.ygyno.2012.06.027.
26. Liu Y, Kim J, Balagurunathan Y, et al. Prediction of pathological nodal involvement by CT-based radiomic features of the primary tumor in patients with clinically node-negative peripheral lung adenocarcinomas. *Med Phys.* 2018;45(6):2518-2526. doi:10.1002/mp.12901.